Available online at www.sciencedirect.com
SCIENCE DIRECT®
Biochimica et Biophysica Acta 1616 (2003) 137–146
BIOCHIMICA ET BIOPHYSICA ACTA
BBA
www.bba-direct.com

Plasmalogens protect unsaturated lipids against UV-induced oxidation in monolayer

Sandrine Morandat[a,*], Muriel Bortolato[a], Geneviève Anker[b], Alain Doutheau[c], Michel Lagarde[b], Jean-Paul Chauvet[d], Bernard Roux[a]

[a] *Laboratoire de Physico-Chimie Biologique, UMR-CNRS 5013, Bât. E. Chevreul, Université Claude Bernard Lyon I, 43 Bd du 11 Novembre 1918, F-69622 Villeurbanne Cedex, France*
[b] *Laboratoire de Biochimie et Pharmacologie, INSERM U352, Bât. L. Pasteur, INSA de Lyon, 20 Av. A. Einstein, F-69621 Villeurbanne Cedex, France*
[c] *Laboratoire de Chimie Organique, UMR-CNRS 5622, Bât. J. Verne, INSA de Lyon, 20 Av. A. Einstein, F-69621 Villeurbanne Cedex, France*
[d] *Laboratoire d'Ingénierie et de Fonctionnalisation des Surfaces, UMR-CNRS 5621, Equipe Bioingénierie et Reconnaissance Génétique, Ecole Centrale de Lyon, 36 Av. G. de Collongue, F-69134 Ecully Cedex, France*

Received 28 January 2003; received in revised form 11 June 2003; accepted 12 August 2003

Abstract

Oxidative stress results from the attack by free radicals of several cellular targets (proteins, DNA and lipids). The cell equilibrium is a direct consequence of the pro-/antioxidant balance. In order to understand the physiological processes involved in oxidative stress, we followed oxidation of unsaturated lipids using a biomimetic system: Langmuir monolayers. The oxidation mode chosen was UV-irradiation and the lipid model was a polyunsaturated phospholipid: 1,2-dilinoleoyl-*sn*-glycero-3-phosphocholine (DLPC). The monomolecular film technique was used to measure membrane rheology before and after UV-irradiation. We showed that the UV-irradiation of a DLPC monomolecular film led to a molecular area and surface elasticity modulus decrease that attests to the apparition of new molecular species at the air–water interface. The antioxidant effect of a synthetic plasmalogen (1-*O*-(1′-(*Z*)-hexadecenyl)-2-*O*-oleoyl-*sn*-glycero-3-phosphocholine or P_{PLM}OPE) was tested on the oxidation of DLPC. Indeed, for about 25% mol P_{PLM}OPE in mixed DLPC/P_{PLM}OPE monolayers, a complete inhibition of the molecular area and the surface elasticity modulus decreases was observed in our experimental conditions. Lower P_{PLM}OPE quantities delayed but did not prevent the DLPC oxidation in mixed monolayers.

Keywords: Monolayer; Plasmalogen; UV; Unsaturated lipid oxidation; Antioxidant

1. Introduction

Peroxidative damages of membrane lipids are a common consequence of free radical-mediated chain reaction. In living systems, it is associated with several physiopathological events (e.g. atherosclerosis, cancer, ageing, neurodegenerative diseases,...). These medical consequences of cellular damage have motivated the investigations in the mechanism of lipid peroxidation, but also in the protective role of antioxidants in membrane model systems.

Peroxidation of unsaturated acyl residues by ionizing radiation in the presence of oxygen, induces the formation of hydroperoxide and acyl chain cross-linkage [1]. UV light is commonly used in the food industry to reduce microbial growth. But this can affect food quality by inducing photooxidation of polyunsaturated fatty acids [2]. Indeed, UV light induces the formation of reactive oxygen species such as superoxide anion, singlet oxygen and peroxyl radicals [3]. An UVC irradiation at 254 nm of a linoleic acid emulsion exhibits the formation of lipid peroxides [2]. The formation of thiobarbituric acid reactive substances (TBARS) is induced by UVA (320–400 nm) as shown in liposomes [4,5] as well as in cultured human skin fibroblasts [6,7].

Different molecules can assume protection against oxidative stress: vitamin E, cholesterol and plasmalogens are some examples [8–10]. Plasmalogens describe a peculiar class of membrane glycerophospholipids that display a unique structural feature: a vinyl-ether linkage at the *sn*-1 position instead

Abbreviations: DLPC, 1,2-dilinoleoyl-*sn*-glycero-3-phosphocholine; DLPE, 1,2-dilinoleoyl-*sn*-glycero-3-phosphoethanolamine; DMPC, 1,2-dimyristoyl-*sn*-glycero-3-phosphocholine; Ks, surface elasticity modulus; POPE, 1-palmitoyl, 2-oleoyl-*sn*-glycero-3-phosphoethanolamine; P_{PLM}OPE, 1-*O*-(1′-(*Z*)-hexadecenyl)-2-*O*-oleoyl-*sn*-glycero-3-phosphocholine

* Corresponding author. Tel.: +33-4-7243-1542; fax: +33-4-7243-1543.
E-mail address: morandat@univ-lyon1.fr (S. Morandat).

0005-2736/$ - see front matter © 2003 Elsevier B.V. All rights reserved.
doi:10.1016/j.bbamem.2003.08.001

of the usual ester linkage. They are widely distributed in animals [11] as well as in certain anaerobic microorganisms. The most abundant form is plasmenylethanolamine. Significant levels of plasmenylcholine were also found especially in cardiac tissue [12].

While the proportion of plasmalogens is relatively high in heart, striated muscle, nervous tissues, and inflammatory and immunological cells, their precise biochemical role in the lipid bilayer has remained elusive for a long time. As they are also linked with certain pathologies and with human genetic disorders, interest for these molecules has been stimulated. Plasmalogens have been suggested as a storage terminal for polyunsaturated fatty acids in order to maintain high levels of these acids in some tissues [11,13]. The cellular pool of arachidonic acid is mostly concentrated in plasmenylethanolamine [11]. The oxidation of plasmenyl arachidonoyl phospholipids leads to the formation of esterified arachidonate oxidized at carbon 5 that are cleaved by the phospholipase A2 action. These products liberated as free acids are eicosanoids that mediate and regulate biochemical events [13]. This is particularly true for macrophages and neutrophils that have high levels of plasmalogens and respond to a variety of stimuli to form and release arachidonic acid. Moreover, plasmalogens are an important precursor of Platelet-Activating Factor [14]. As membrane components, plasmalogens form non-bilayer structures, due to the presence of the vinyl-ether double bond [10]. This promotes membrane–membrane fusions and membrane ion linkages, and this may be important in some biological events as endocytosis and secretion. The hypothesis that plasmalogens act as singlet oxygen quencher is supported by the ability of reactive oxygen species to abstract the hydrogen in α position. As antioxidant, plasmalogens appeared to be a target for oxidative damage [15,16]. Studies on multilamellar liposomes and LDL presented the inhibitory effect of plasmalogens on iron- and copper-dependent lipid peroxidation [17,18] and on AAPH oxidation [16,19].

The aim of our work is to investigate the effect of plasmalogens on the UV-oxidation of a polyunsaturated phospholipid in monolayers. The monolayer technique is a powerful method for studying enzymatic [20] and non-enzymatic reactions [21]. It is possible to get useful molecular information on the behavior of the unsaturated lipids after UV exposure, i.e. to characterize the physical properties of membrane after oxidative stress. The antioxidant role of plasmalogens was often studied with cellular extracts [18], in cells directly [22] or with liposomes [17] but never with monolayers.

2. Materials and methods

2.1. Materials

1,2-dilinoleoyl-*sn*-glycero-3-phosphocholine (DLPC) and 1,2-dimyristoyl-*sn*-glycero-3-phosphocholine (DMPC) were purchased from Sigma Chemicals (St. Louis, MO, USA). L-2,3-*O*-isopropylidene-*sn*-glycerol was obtained from Aldrich (France). All other chemicals and reagents were of the highest purity available from Merck (Darmstadt, Germany) and from Aldrich. All solvents were of chromatographic grade. The DLPC solution was protected against light and stored in a freezer until spreading. The distilled water was purified with a Millipore MilliQ filtering system, yielding a water resistance of 18.2 MΩ × cm.

2.2. Synthesis of the plasmalogen (P_{PLM}OPE)

The P_{PLM}OPE was synthesized as follows. Commercially available L-2,3-*O*-isopropylidene-*sn*-glycerol was acylated with palmitoyl chloride (Pyr., CH_2Cl_2; 95%) to give 1-*O*-Palmitoyl-2,3-*O*-isopropylidene-*sn*-glycerol. The isopropylidene protective group was then removed (MeOH, HCl; 74%) yielding 1-*O*-palmitoyl-*sn*-glycerol which was then transformed into 3-*O*-(*tert*-butyldiphenylsilyl)-1-*O*-(1′-(*Z*)-hexadecenyl)-*sn*-glycerol, in about 50% overall yield, according to the five-step Thompson's sequence [23]. Acylation with oleoyl chloride (Pyr., CH_2Cl_2; 91%) afforded 3-*O*-(*tert*-butyldiphenylsilyl)-1-*O*-(1′-(*Z*)-hexadecenyl)-2-*O*-oleoyl-*sn*-glycerol. Removal of the *tert*-butyldiphenylsilyl group (Bu_4NF/THF; 85%) led to 1-*O*-(1′-(*Z*)-hexadecenyl)-2-*O*-oleoyl-*sn*-glycerol[1] which was reacted with 2-azidoethyl dichlorophosphate[2] according to the procedure of Pfaendler and Weimar [24] to give rise, after hydrolysis, to 3-*O*-[2-azidoethoxy(hydroxy)phosphoryl]-1-*O*-(1′-(*Z*)-hexadecenyl)-2-*O*-oleoyl-*sn*-glycerol in 70% yield. Finally, reduction of the azide function [24] (PPh_3, THF/H_2O; 67%) furnished 1-*O*-(1′-(*Z*)-hexadecenyl)-2-*O*-oleoyl-*sn*-glycero-3-phosphocholine.

Melting points were determined with a Kofler hot-stage melting-point apparatus. Optical rotations were measured with a Perkin-Elmer 241 polarimeter. IR spectra were recorded in $CHCl_3$, except when otherwise stated, on a Perkin-Elmer 1310 spectrometer. ^{1}H NMR and ^{13}C NMR spectra were recorded in $CDCl_3$ with a Bruker AM 200 spectrometer. Chemical shifts are given in ppm downfield from internal Me_4Si. Splitting patterns abbreviations are: s, singulet; se, broad singulet; d, doublet; t, triplet; q, quartet; m, multiplet; p, pseudo. Mass spectra (HMRS) were recorded with a THERMOFinnigan MT 95XL at the "Centre de Spectrométrie de Masse de l'Université Claude Bernard Lyon 1".

2.2.1. 1-O-Palmitoyl-2,3-O-isopropylidene-sn-glycerol

Colourless solid with a low melting point. $[\alpha]_D^{25}$-0.54 (c 10, $CHCl_3$). IR: 1730. ^{1}H NMR: δ 0.90 (3H, t, J = 7 Hz); 1.25 (24 H, se); 1.37 (3H, s); 1.45 (3H, s); 1.60 (2H, m); 2.35 (2H, t, J = 7 Hz); 3.70 (1H, dd, J = 8, J = 6 Hz); 4.10 (3H, m); 4.40 (1H, m).

[1] Thin-layer chromatography revealed the formation of a few amount of the isomer resulting from the migration of the acyl chain from *sn*-2 to *sn*-1 position which was eliminated during chromatography.

[2] This reagent was used freshly prepared and passed (CH_2Cl_2) through a short column of silica gel.

2.2.2. 1-O-Palmitoyl-sn-glycerol

Colourless solid. $P_F = 73-75$ °C. $[\alpha]_D^{25}$-6.52 (c 1.5, $CHCl_3$). IR 3560, 3440, 1720. ^{1}H NMR: δ 0.9 (3H, t, J = 7 Hz). m); 1.25 (24H, se); 1.65 (2H, m); 2.40 (2H, t, J = 7 Hz); 3.65 (1H, dd, J = 11, J = 4 Hz); 4.10 (3H, m); 4.20 (1H, m). ^{13}C NMR: δ 14.14 (q), 22.72 (t), 24.95 (t), 29.17 (t), 29.29 (t), 29.39 (t), 29.49 (t), 29.64 (t), 29.69 (t), 29.72 (t), 31.96 (t), 34.20 (t), 63.41 (t), 65.18 (t), 70.32 (d), 174.40 (s). ^{1}H and ^{13}C NMR data in accordance with literature [25].

2.2.3. 3-O-(tert-Butyldiphenylsilyl)-1-O-(1′-(Z)-hexadecenyl)-sn-glycerol

Light yellow oil. IR_{film} 1660. ^{1}H NMR: δ 0.88 (3H, t, J = 7Hz); 1.05 (9H, s); 1.25 (24H, se); 2.00 (2H, m); 2,50 (OH, se); 3.70 (m, 5H); 4.35 (1H, m); 5.95 (1H, dt, J = 6.2, J = 1.4 Hz); 7.30 (6H, m); 7.70 (4H, m). In accordance with literature data [23]. ^{13}C NMR: δ 14.12 (q), 22.69 (t), 23.93 (t), 26.6 (s), 26,84 (t), 29.32 (t), 29.37 (t), 29.54 (t), 29.67 (t), 29.71 (t), 29.76 (t), 31.93 (t), 64.39 (t), 70.64 (d), 72.46 (t), 107.69 (d), 127.63 (d), 127.78 (d), 129.51(d), 129.81 (d), 134.84 (d), 135.52 (d), 144.82 (d).

2.2.4. 3-O-(tert-Butyldiphenylsilyl)-1-O-(1′-(Z)-hexadecenyl)-2-O-oleoyl-sn-glycerol

Light yellow oil. $[\alpha]_D^{25}$-0.17 (c 3.5, $CHCl_3$). IR_{film}: 1735, 1660.^{1}H RMN: δ 0.89 (6H, m); 1.06 (9H, s); 1.26 (46H, se); 1.6 (2H, m); 2.01 (4H, m); 2.3 (2H, m); 3.81 (2H, ABX, J = 11.34, J = 4.86 Hz); 3.95 (2H, ABX, J = 5.2 Hz); 4.35 (1H, pq, J = 7 Hz); 5.12 (1H, m); 5.36 (2H, m); 5.92 (1H, dt, J = 6.24, J = 1.5 Hz); 7.45 (m, 6H); 7.65 (m, 4H). ^{13}C NMR: δ 14.12 (q), 19.25 (s), 22.70 (t), 23.91 (t), 24.92 (t), 26.74 (t), 27.20 (t), 29.13 (t), 29.22(t), 29.34 (t), 29.38 (t), 29.54 (t), 29.59 (t), 29.73 (t), 31.92 (t), 34.39 (t), 27.23 (q), 62.21 (t), 69.95 (t), 72.59 (d), 107.72 (d), 127.72 (d), 129.74 (d), 129.97 (d), 133.17 (s), 133.22 (s), 135.52 (d), 135.57 (d), 144.89 (d), 173.01 (s).

2.2.5. 1-O-(1′-(Z)-Hexadecenyl)-2-O-oleoyl-sn-glycerol

Light yellow oil rapidly used in the next step. ^{1}H RMN: δ 0.89 (6H, m); 1.29 (46H, se); 1.62 (2H, m); 1.9–2.1 (4H, m); 2.39 (2H, m); 3.80–3.90 (4H, m); 4.39 (1H, pq, J = 7.3 Hz); 5.04 (1H, m); 5.35 (2H, m); 5.91 (1H, dt, J = 6.2, J = 1.3 Hz).^{13}C NMR: δ 14.15 (q), 20.84–34.38 (14 CH_2), 62.12 (t), 70.20 (t), 73.09 (d), 108.3 (d), 129.75 (d), 130.05 (d), 144.59 (d), 173.58 (s).

2.2.6. 3-O-[2-Azidoethoxy(hydroxy)phosphoryl]-1-O-(1′-(Z)-hexadecenyl)-2-O-oleoyl-sn-glycerol

Light yellow oil. $[\alpha]_D^{25}$-1 (c 1.5, $CHCl_3$). IR: 2910, 2850, 2110, 1725, 1660, 1450, 1375, 1345. ^{1}H RMN: δ 0.88 (6H, m); 1.32 (46H, se); 1.60 (2H, m); 2.02 (4H, m); 2.30 (2H, t, J = 7.5 Hz); 3.40 (2H, m); 3.95 (2H, m) 4.10 (4H, m); 4.32 (1H, pq, J = 6.1 Hz); 5.17 (1H, m); 5.34 (2H, m); 5.89 (1H, dt, J = 6.1, J = 1.4 Hz); 11.07 (1H, OH). ^{13}C NMR: δ 14.14 (q), 22.69 (t), 23.97 (t), 27.24 (t), 29.34 (t), 29.38 (t), 29.55 (t), 29.78 (t), 31.94 (t), 51.40 (t), 63.83 (t), 64.52 (t), 70.24 (t), 71.52 (d), 107.79 (d), 129.77 (d), 130.01 (d), 144.83 (d), 173.23 (s). FAB HMRS (-$FAB_{M=M-1}$) m/z = calculated for $C_{39}H_{73}N_3O_7P$ 726.5186, found: 726.5205.

2.2.7. 1-O-(1′-(Z)-Hexadecenyl)-2-O-oleoyl-sn-glycero-3-phosphoethanolamine (P_{PLM}OPE)

Light yellow oil. $[\alpha]_D^{25}$-0.6 (c 2, $CHCl_3$). IR: 2900, 2850, 1725, 1655, 1450, 1370. ^{1}H RMN: δ 0.88 (6H, m), 1.26 (46H, se); 1.6 (m, 2H); 2.0 (4H, m); 2.31 (2H, t, J = 7.4 Hz); 3.14 (2H, m); 3.92 (4H, m); 4.07 (2H, m); 4.33 (1H, pq, J = 7 Hz); 5.15 (1H, m); 5.34 (2H, m); 5.90 (1H, d, J = 6.1 Hz); 8.45 (3H, NH_2, OH). ^{13}C NMR: δ 14.13 (q), 22.77 (t), 23.99 (t), 24.66 (t), 25.00 (t), 27.27 (t) 29.23 (t), 29.27 (t), 29.38 (t), 29.43 (t), 29.47 (t), 29.59 (t), 29.74 (t), 29.82 (t), 31.96 (t), 31.98 (t), 34.39 (t), 40.47 (t), 62.15 (t), 63.82 (t), 70.25 (t), 71.37 (d), 107.87 (d), 129.71 (d), 130.01 (d), 144.77 (d), 173.67 (s). FAB HMRS (-$FAB_{M=M-1}$) m/z = calculated for $C_{39}H_{75}NO_7P$ 700.5281, found: 700.5280, structure represented in Scheme 1.

2.3. Monolayer technique

All experiments were performed at constant temperature (21 ± 0.1 °C), protected from ambient light and under nitrogen saturated atmosphere. The film balance was built by R&K (Riegler and Kirstein, Wiesbaden, Germany) and equipped with a Wilhelmy-type surface-pressure measuring system. The subphase was 150 mM KCl, 10 mM Tris–HCl pH 7.2 buffer (TBS).

Phospholipids were spread at the air–water interface in hexane/ethanol 9:1 (v/v) to reach a final quantity of about 19 nmol of lipids. The solvent was allowed to evaporate for 20 min prior to compression. Then, the monolayer was compressed at 6 cm^2/min up to a lateral pressure of 33 mN/m to obtain a pressure–area isotherm (π–A isotherm). All lipid mixtures were used immediately after their preparation.

The limiting molecular area of molecules was estimated by extrapolating the condensed-like curve to zero surface pressure.

The calculated ideal molecular area (A_{ideal}) of two-component mixtures was determined at a given surface pressure using the following equation:

$$A_{ideal} = x_1 A_1 + (1 - x_1) A_2$$

where x_1 is the mol fraction of component 1 and (A_1) and (A_2) are the molecular areas at a π pressure of pure components 1 and 2, respectively. Deviations of the experimental A_{ideal} values from the sum of the contributions of the pure lipids indicate a non-ideal behavior of the lipid mixture in the mixed monolayers. Negative deviations from the sum of the contributions are indicative of area condensation and imply an intermolecular attraction between the lipids in the mixed films [26,27].

The surface elasticity moduli (Ks) were calculated from the pressure–area data obtained from the monolayer compressions using the following equation [28]:

$$\mathrm{Ks} = -A\left(\frac{\mathrm{d}\pi}{\mathrm{d}A}\right)$$

where A is the molecular area at the indicated surface pressure π.

High Ks values correspond to low interfacial fluidity among packed lipids forming a monolayer. This suggests that the higher the Ks value of a monolayer is, the more difficult it is to deform it.

At a given lipid mixing ratio, an ideal Ks^{-1} behavior can be determined by imparting a specific contribution of the Ks^{-1} value of each pure lipid on the reciprocal elasticity coefficient, depending on both molecular area fraction and mole fraction parameters [29]. Thus, at a given constant surface pressure, the ideal Ks^{-1} can be defined by the following equation:

$$\mathrm{Ks}^{-1}_{12} = \left(\frac{1}{A_{\mathrm{ideal}}}\right)[(\mathrm{Ks}_1^{-1} \times A_1)x_1 + (\mathrm{Ks}_2^{-1} \times A_2)(1 - x_1)]$$

where x_1 is the mol fraction of component 1 and (A_1) and ($\mathrm{Ks}^{-1}{}_1$) or (A_2) and ($\mathrm{Ks}^{-1}{}_2$) are the molecular areas and surface elasticity moduli of pure components 1 and 2, respectively. Deviations of the experimental Ks^{-1} values from the additivity of the pure lipid contributions indicate a non-ideal behavior of the lipidic mixture in the mixed monolayers.

After recording the π–A isotherm, the monolayer was stabilized 10 min at 30 mN/m fixed surface pressure to mimic the internal pressure of biological membranes [30]. Oxidation was performed by lipid monolayer UV-irradiation with a Vilber Lourmat 50 W lamp (254 nm emission maximum and 7 mW/cm^2 fluence rate). The monitoring period was about 180 min including various irradiation time periods. After recording the molecular area variation, a final π–A isotherm was recorded. The molecular area value at 30 mN/m surface pressure ($A_{30\ \mathrm{mN/m}}$) after 180 min monitoring was determined and it was subtracted to the $A_{30\ \mathrm{mN/m}}$ before the UV-irradiation ($\Delta A_{30\ \mathrm{mN/m}}$).

3. Results

3.1. Effect of UV-irradiation on the physical properties of DLPC and P_{PLM}OPE monolayers

The structure of the plasmalogen used for this study was depicted in Scheme 1. Fig. 1A showed the DLPC (curve 1) and P_{PLM}OPE (curve 2) isotherms measured under the conditions described in Materials and methods. It may be seen that both lipids give a stable monolayer since they could be compressed to surface pressures greater than 30 mN/m. As one can see, the DLPC and P_{PLM}OPE limiting molecular areas were located around 90 Å^2/molecule and 62 Å^2/molecule, respectively. The P_{PLM}OPE limiting molecular area value is different from that obtained for the corresponding acylated phospholipid (1-palmitoyl, 2-oleoyl-*sn*-glycero-3-phosphoethanolamine or POPE) (data not shown). As the POPE limiting molecular area is 77 Å^2/molecule under the same conditions, this clearly demonstrates that the vinyl-ether function of P_{PLM}OPE molecules induced a more condensed bidimensional molecular arrangement at the air–water interface.

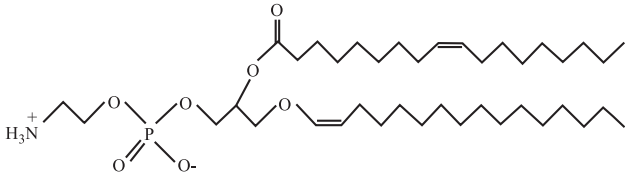

Scheme 1.

An estimation of the surface elasticity modulus (Ks) of these monolayers is presented Fig. 1B. The Ks values at 30 mN/m surface pressure were located around 95 and 140 mN/m for DLPC and for P_{PLM}OPE, respectively. These two Ks values are characteristic of a common phospholipid monolayer. Nevertheless, the P_{PLM}OPE Ks indicated a more rigid film than that of DLPC.

Because it has been shown that the physical close packing of the unsaturated lipid molecules enhances propagation of oxidative process [31], the surface pressure was fixed at 30 mN/m and each monolayer was UV-irradiated during 180 min. Then, the resulting monomolecular films were decompressed and new π–A isotherms were recorded (Fig. 1A, curve 1′ and 2′). For DLPC, the comparison between curve 1 and 1′ showed clearly that the UV-irradiation led to a dramatic decrease of the limiting molecular area: 90 Å^2/molecule for DLPC and 67 Å^2/molecule for the irradiated DLPC derivatives. For the P_{PLM}OPE film, the π–A isotherm obtained after the UV-irradiation presented an extrapolated limiting molecular area at about 60 Å^2/molecule. A similar low decrease of the extrapolated limiting molecular area was obtained with a non-oxidizable phospholipid, DMPC (data not shown). This low molecular area decrease might be linked to the subphase evaporation and/or to the molecular rearrangement of the lipid at the interface. In these conditions, the π–A isotherms obtained before and after UV-irradiation of P_{PLM}OPE did not present a significant molecular area variation.

The Ks of these irradiated monolayers are presented Fig. 1B. As one can see, for DLPC, the UV-irradiation led to a dramatic decrease of the Ks value, at 30 mN/m surface pressure: changing from 95 mN/m for non-irradiated DLPC monolayer (curve 1) to 58 mN/m for a DLPC irradiated monolayer (curve 1′). This Ks value attests the

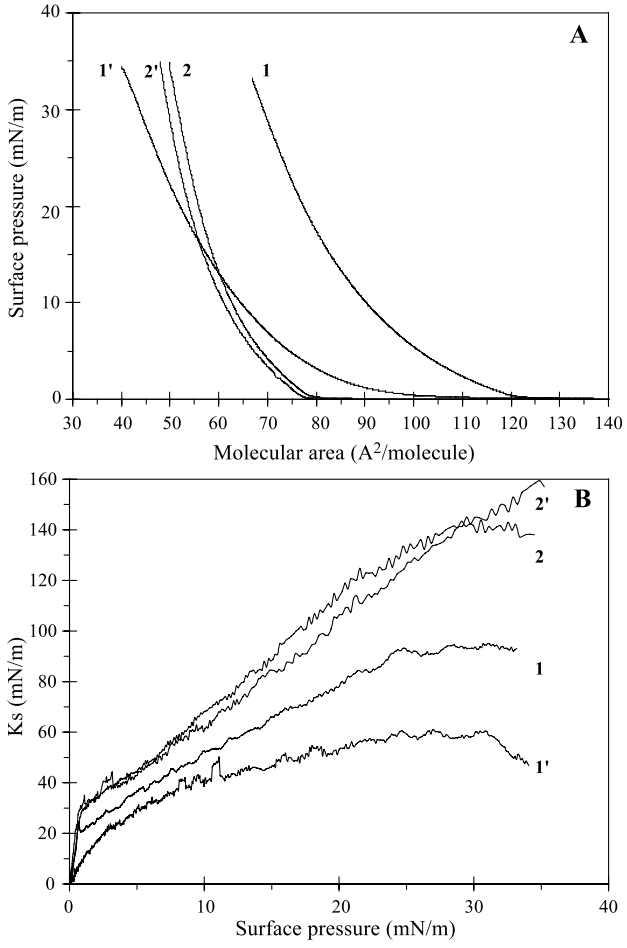

Fig. 1. $\pi-A$ isotherm and variation of Ks with pressure of DLPC and P_{PLM}OPE monolayers before and after UV-irradiation. 19.2 nmol of each lipid were spread at the air–water interface and after solvent evaporation the $\pi-A$ isotherms were measured (A); (1), DLPC and (2), P_{PLM}OPE. The surface pressure of each monolayer was fixed at 30 mN/m and after stabilization, an UV-irradiation was realized during 180 min. Then, the film was decompressed and after 15 min at 0 mN/m, new $\pi-A$ isotherms were measured; isotherm 1′: 180-min irradiated DLPC and isotherm 2′: 180-min irradiated P_{PLM}OPE. From these $\pi-A$ isotherms, the monolayer Ks were calculated and represented as a function of surface pressure (B); (1), DLPC; (2), P_{PLM}OPE; (1′), 180-min irradiated DLPC and (2′), 180-min irradiated P_{PLM}OPE. The atmosphere was nitrogen-saturated and the experiment was performed protected from light. The subphase buffer was 10 mM Tris–HCl, 150 mM KCl pH 7.2, thermostated at 21 °C. Each experiment were repeated at least two times.

formation of a more fluid film. The variation of limiting molecular area and Ks could be due to the formation of new molecular species at the air–water interface during the irradiation period because UV-irradiation is known to promote lipid peroxidation in various experimental systems [2,4]. In order to evidence the apparition of new molecular species at the air–water interface, irradiated DLPC monolayers were extracted with chloroform and the organic phases containing the lipids were then deposited on TLC plate (data not shown). The complete disappearance of the DLPC was observed, this seems to confirm the production of new molecular species from an UV-irradiated DLPC monolayer. Further analysis of these species cannot be realized because of the complexity of the product mixture.

For P_{PLM}OPE monolayers, the Ks values before and after UV-irradiation were about the same (140 mN/m). This indicates that the P_{PLM}OPE monolayer physical properties were not changed by the UV-irradiation.

As controls, a DLPC monolayer maintained at 30 mN/m surface pressure without UV exposure and under a saturated oxygen atmosphere presented no molecular area decrease. Indeed, the isotherm after oxygen exposure was identical to the non-irradiated DLPC one. So, the limiting molecular area decrease observed for the UV-irradiation is the direct consequence of the irradiation and cannot be induced by the presence of oxygen molecules either in the gaseous phase or dissolved in the subphase buffer.

3.2. Monitoring of the UV-induced oxidation of DLPC and P_{PLM}OPE monolayers

The variations of the DLPC and P_{PLM}OPE monolayers molecular area at 30 mN/m during the 180 min UV-irradiation were recorded and plotted versus time (Fig. 2). For the DLPC, the first UV-irradiation minutes exhibited a plateau. Then, a rapid molecular area decrease appeared 30 min after the beginning of the monitoring. The total molecular area diminution at 30 mN/m after 180 min UV-irradiation reached 28 Å^2/molecule. This clearly shows that the UV-oxidation of DLPC monolayers led to an important molecular area decrease. For the P_{PLM}OPE monolayer, no significant molecular area variation was observed. It seems that the UV-irradiation have no effects on this phospholipid.

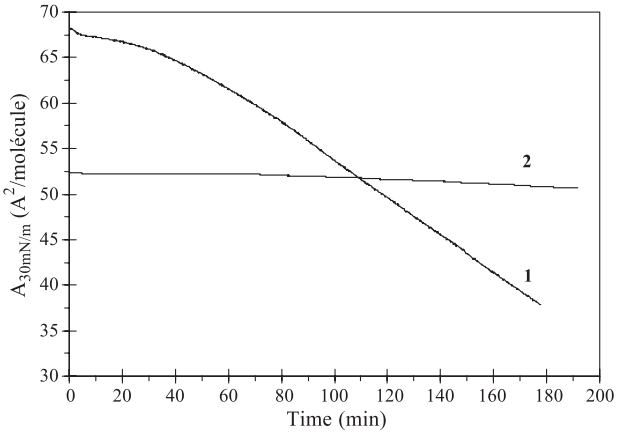

Fig. 2. Monitoring of the molecular area variation induced by 180 min UV-irradiation at 30 mN/m. Lipids (19.2 nmol) were spread at the air–water interface. After solvent evaporation, the $\pi-A$ isotherm was measured. The monolayer was UV-irradiated for 180 min at 30 mN/m surface pressure. The molecular area variation was recorded with time for DLPC (1) and for P_{PLM}OPE (2). The atmosphere was nitrogen-saturated and all experiments were performed protected from light. The subphase buffer was 10 mM Tris, 150 mM KCl pH 7.2, thermostated at 21 °C. Each experiment were repeated at least two times.

This showed that the vinyl-ether bond was not affected by this UV-exposure because the P_{PLM}OPE monolayer properties (molecular area and fluidity) were recovered after this treatment. As control, the molecular area variation of a 180 min UV-irradiated DMPC monolayer was recorded and it showed a molecular area decrease that was not significant (data not shown). These results also mean that the molecular area decrease observed in the case of an irradiated DLPC monolayer was not due to the cleavage of the ester bond or of the headgroup.

3.3. Influence of the UV-irradiation time on DLPC oxidation

The effect of irradiation time on DLPC oxidation was shown in Fig. 3A. After stabilization of monolayers at 30 mN/m surface pressure, DLPC was UV-irradiated during different times: 5, 15, 30 and 180 min curves 1, 2, 3 and 4, respectively. A control was realized with a DLPC monolayer that was not UV-irradiated. The molecular area decrease was represented versus time (Fig. 3A). As one can see, the longer the UV-irradiation was, the more important the molecular area decrease was. This experiment also showed that 5, 15 and 30 min UV-irradiation appears as a suitable delay to induce a sufficient molecular area decrease even after the UV light suppression.

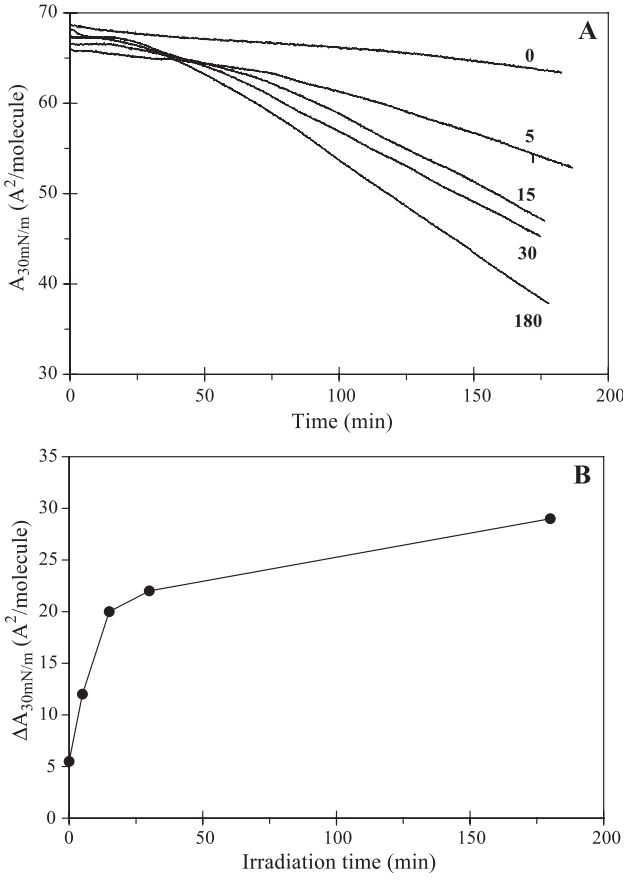

Fig. 3. Influence of irradiation time on DLPC molecular area variation. DLPC (19.2 nmol) were spread at the air–water interface. After stabilization at 30 mN/m surface pressure, the UV-irradiation was carried out during various times. A control was realized with a DLPC monolayer that was not UV-irradiated (0). The different irradiation times used were (5), 5 min; (15), 15 min; (30), 30 min and (180), 180 min. The atmosphere was nitrogen-saturated and all experiments were performed in darkness. The subphase buffer was 10 mM Tris–HCl, 150 mM KCl pH 7.2, thermostated at 21 °C. Each experiment were repeated at least two times.

The $\Delta A_{30\ mN/m}$ was calculated for each molecular area decrease and it was plotted versus the irradiation delay (Fig. 3B). This figure showed a rapid $\Delta A_{30\ mN/m}$ increase between 0 and 15 min UV-irradiation and then a slower $\Delta A_{30\ mN/m}$ increase between 15 and 180 min. Fifteen- and thirty-minute UV-irradiation exhibited about the same $\Delta A_{30\ mN/m}$ than 180 min, which is why, in the following, only 15- and 180-min UV-irradiation will be used.

3.4. Physical properties of mixed DLPC/P_{PLM}OPE monolayers

Mixtures containing different molar ratios (from 10% to 30%) of P_{PLM}OPE over DLPC were spread at the air–water interface and the corresponding isotherms were recorded (Fig. 4A). The molecular areas at 10, 20 and 30 mN/m surface pressures and the Ks values at 30 mN/m surface pressure were determined. The A_{ideal} of each mixture was calculated and these results were represented in Fig. 4B. Theoretical and calculated Ks values at 30 mN/m ($Ks_{30\ mN/m}$) surface pressure were determined for all percentages. Fig. 4C shows the difference between the calculated $Ks_{30\ mN/m}$ and the theoretical $Ks_{30\ mN/m}$ ($\Delta Ks_{30\ mN/m}$) plotted versus the molar percentage of P_{PLM}OPE. Because P_{PLM}OPE had a lower limiting molecular area than DLPC, increasing its molar percentage in the monolayer leads to the limiting molecular area decrease (Fig. 4A). Moreover, the limiting molecular areas values determined experimentally were not quite different from those calculated as ideal (Fig. 4B). So the behavior of the bidimensional mixture can be considered as ideal. The $\Delta Ks_{30\ mN/m}$ were calculated and it showed that the monolayer was more fluid than expected. Indeed, because the $\Delta Ks_{30\ mN/m}$ values were not great, the Ks variations between the Ks determined experimentally and those ideal were negligible (Fig. 4C), this confirms that the mixture behaves as an ideal mixture.

3.5. Monitoring of the UV-induced oxidation of mixed DLPC/P_{PLM}OPE monolayers

DLPC mixed monolayers containing 10%, 20% or 30% mol DMPC or 10%, 15%, 20%, 25%, 28% or 30% mol P_{PLM}OPE were formed at the air–buffer interface. The monolayers were stabilized at 30 mN/m surface pressure and the UV-irradiation was carried out during 15 min. The $\Delta A_{30\ mN/m}$ were determined for each experiment and were plotted versus DMPC or P_{PLM}OPE molar percentage (Fig. 5A). Moreover, the lag time of each molecular area

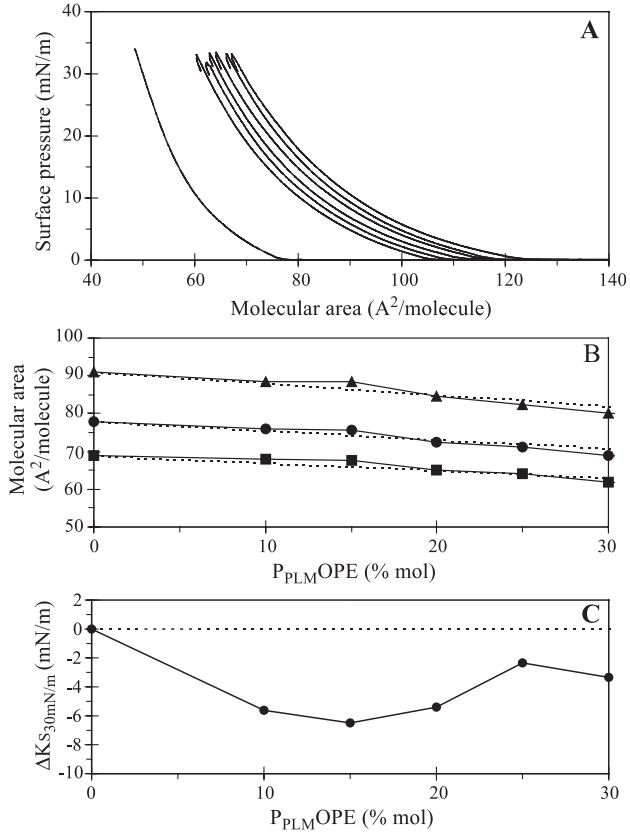

Fig. 4. DLPC/P_{PLM}OPE mixed monolayers, $\pi-A$ isotherms and ideality. Mixed DLPC/P_{PLM}OPE (19.2 nmol) were spread at the air–water interface and after solvent evaporation, the $\pi-A$ isotherms were recorded (A). The P_{PLM}OPE percentages in the monolayer were, from right to left, 0%, 10%, 15%, 20%, 25%, 30% and 100%. From each $\pi-A$ isotherm, the molecular area at 10 (triangles), 20 (circles) and 30 mN/m (squares) were plotted versus the molar percentage of P_{PLM}OPE (B). The dashed lines correspond to ideal 2D mixing of the components at each surface pressures. The Ks values determined for each mixture at 30 mN/m surface pressure minus theoretical Ks values at the same pressure ($\Delta Ks_{30\ mN/m}$) plotted versus molar percentage of P_{PLM}OPE (C). The atmosphere was nitrogen-saturated and all experiments were performed protected from light. The subphase buffer was 10 mM Tris–HCl, 150 mM KCl pH 7.2, thermostated at 21°C. These results correspond to the average of at least two experiments.

decrease was calculated and represented in Fig. 5B. For both DMPC and P_{PLM}OPE containing monolayers, increasing amounts of DMPC or P_{PLM}OPE induced a decreasing $\Delta A_{30\ mN/m}$. For 10% mol P_{PLM}OPE the $\Delta A_{30\ mN/m}$ was not quite different from those obtained with 10% mol DMPC. For the DMPC-containing films, the $\Delta A_{30\ mN/m}$ decreased quasi-linearly, whereas for the P_{PLM}OPE one, a rapid decrease was observed for 15% and 20% mol P_{PLM}OPE. The $\Delta A_{30\ mN/m}$ reached about 2 Å^2/molecule for 25%, 28% and 30% mol P_{PLM}OPE monolayers. This clearly demonstrates that the P_{PLM}OPE molecules were able to prevent DLPC oxidation because the molecular area decrease is negligible from 25% mol.

The lag time for short-time UV-irradiations was determined. Fig. 5B shows the difference between the lag time for 15 min UV-irradiation of mixed monolayers and the lag time for 15 min UV-irradiation of a DLPC monolayer (corrected lag time) plotted versus the P_{PLM}OPE molar percentage. DMPC monolayer (10% mol) presented about the same corrected lag time as DLPC alone. For the P_{PLM}OPE containing monolayers, the corrected lag time of the reaction was always higher than for the DMPC mixed monolayers. But this difference is more important for 25%, 28% and 30% mol P_{PLM}OPE in the monolayer and was about 150, 460 and 500 min, respectively.

The same experiments were realized with long-time irradiation (180 min) (data not shown). It showed that the P_{PLM}OPE containing monolayers presented about the same $\Delta A_{30\ mN/m}$ than the DMPC one for all the percentages used.

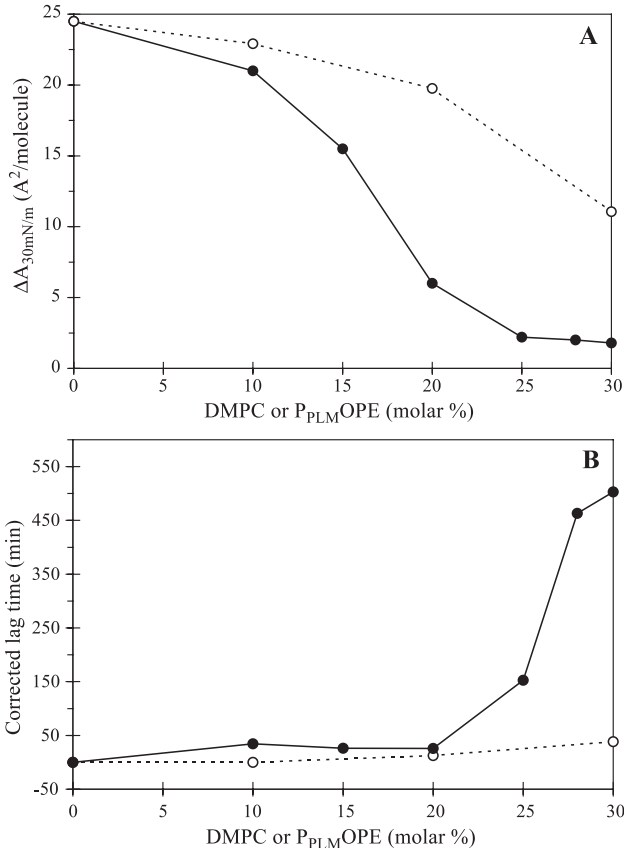

Fig. 5. Effect of P_{PLM}OPE percentage on $\Delta A_{30\ mN/m}$ and lag time after short UV-irradiation time. Mixtures DLPC/P_{PLM}OPE and DLPC/DMPC (19.2 nmol) were spread at the air–water interface. Monolayers were UV–irradiated during 15 min. The amplitude of the normalized molecular area decrease after 180 min was determined ($\Delta A_{30\ mN/m}$). These $\Delta A_{30\ mN/m}$ values were plotted versus the composition of the different mixtures spread (A). The lag time which is the delay preceding a 5% decrease in the apparent molecular area was determined for each mixture (B). Mixtures were DLPC/DMPC, white symbols, dashed lines; and DLPC/P_{PLM}OPE, black symbols, full lines. DMPC molar ratios in DLPC were 10%, 20% and 30% and P_{PLM}OPE ratios were 10%, 15%, 20%, 25%, 28% and 30%. The atmosphere was nitrogen-saturated and all experiments were performed in darkness. The subphase buffer was 10 mM Tris–HCl, 150 mM KCl pH 7.2, thermostated at 21 °C. These results correspond to the average of at least two experiments.

It seems that P_{PLM}OPE had no effects on the DLPC molecular area decrease. However, the 30% mol P_{PLM}OPE-containing monolayer exhibited a corrected lag time 22 min greater than the corresponding DMPC one. This indicates that the P_{PLM}OPE molecules are able to delay DLPC oxidation but not to prevent it.

4. Discussion

From the results above, it is clear that the molecular area decrease of the DLPC is correlated to polyunsaturated fatty acid peroxidation. First, the UV-irradiation is necessary to trigger a decrease in the molecular area, whereas under non-oxidative conditions (under nitrogen-saturated atmosphere, protected from light and absence of UV), the molecular area does not vary significantly within the time of experiments. Second, the presence of a polyunsaturated fatty acid sensitive to the oxidative chain process is required to generate a significant molecular area decrease. Furthermore, the molecular area decrease amplitude ($\Delta A_{30\ mN/m}$) is correlated with UV-irradiation length.

The Langmuir method was chosen because it requires only small amounts of lipids (about 20 nmol) and provides information on the structure of the macromolecular substrate. Indeed, the reaction was monitored in real-time, whereas in previous studies, photooxidation intermediates (peroxides) [2] or final oxidation products such as TBARS [5] were analyzed.

First the physical properties of DLPC and P_{PLM}OPE were determined. The limiting molecular areas of DLPC and P_{PLM}OPE monolayers were 90 and 62 Å^2/molecule, respectively as determined by the π–A isotherm (Fig. 1A). The P_{PLM}OPE limiting molecular area is in agreement with that found by Smaby et al. [32] for ethanolamine plasmalogens. The Ks, deduced from this isotherm, was 140 mN/m at 30 mN/m surface pressure (Fig. 1B). This value is higher than the average Ks of a phospholipid monolayer that is about 100 mN/m at 30 mN/m surface pressure as for a POPE monolayer. Thereby the P_{PLM}OPE monolayer is more rigid than a POPE monolayer. This difference is due to the vinyl-ether function of the P_{PLM}OPE because several studies described that plasmalogens do not exhibit the same behavior in the membrane than diacyl phospholipids. Physicochemistry analysis (e.g. NMR, electron spin resonance) on artificial membranes were realized and it demonstrated that the plasmenylcholine increased the order and the stability of bilayers in respect to phosphatidylcholine [33]. Moreover, the vinyl-ether bond causes a different hydrocarbon side chain conformation at the *sn*-2 acyl chain [34]. In binary mixtures with dioleoyl phospholipids, plasmenylethanolamine exhibits an initial fluidization below 30% (mol%), while above 30%, it exhibits a decrease in fluidity [35].

The 180-min UV-oxidation of DLPC monolayers was characterized by the decrease of the limiting molecular area from 90 Å^2/molecule to 67 Å^2/molecule after 180 min UV-irradiation (Fig. 1A). The di-unsaturated phospholipid DLPC was chosen in order to emphasize the magnitude of the molecular area decrease. The change of limiting molecular area was previously demonstrated by Viitala and Peltonen [21] with dilinoleoylphosphatidylethanolamine (DLPE) using a more condensed phase due to uranyl acetate in the subphase buffer. According to these authors, the UV-irradiation of DLPE monolayer induced a molecular area decrease following (i) a polymerization of lipids of the monolayer during the first 2 min and (ii) the monolayer degradation. Our results showed the direct effect of UV-irradiation on a hemi-membrane of polyunsaturated lipids, by recording the continuous decrease of DLPC molecular area (Fig. 2). It presented a plateau at the initial stage of the oxidation process. This might be due to the propagation time needed by free radicals (generated by the UV-irradiation) to oxidize DLPC.

The oxidation led to the production of many different kind of products [36,37]. The qualitative analysis of these molecules is not straightforward because some of these degradation products were soluble in aqueous phase, such as aldehydes and lysophospholipids. In our study, a Ks decrease at 30 mN/m surface pressure was observed from 95 to 58 mN/m before and after UV-irradiation, respectively (Fig. 1B). This seems to confirm the structural modification described by Viitala and Peltonen [21]. The significance of this Ks decrease observed in Fig. 1B after DLPC UV-irradiation was not totally elucidated. DLPC monolayer fluidity increase was detected after UV-exposure (Fig. 1B). The results about membrane fluidization [38,39] or rigidization [40–42] after oxidation are still very controversial.

The results obtained in Fig. 3 show that the longer the UV-irradiation was, the greater the $\Delta A_{30\ mN/m}$ was. Shih and Hu [5] suggested that preformed hydroperoxides, which are likely to be present in most in vitro membrane systems, might form products that photosensitize to generate singlet oxygen. Singlet oxygen could then react with unsaturated fatty acids and generate peroxyl radicals. So, the number of generated radicals was directly related to the duration of UV-irradiation.

The theoretical limiting molecular area and the average monolayer compressibility of a mixture of two components were calculated according to Smaby et al. [29]. These parameters showed that the mixture of these two components was ideal (Fig. 4). This suggests that the P_{PLM}OPE molecules were not organized in domains within the DLPC monolayer. Since P_{PLM}OPE is homogeneously mixed to DLPC within the monolayer, it might be an efficient antioxidant.

No significant molecular area decrease was observed when a pure P_{PLM}OPE monolayer was irradiated (Fig. 2). This confirms the results obtained by Reiss et al. [16], which evidenced that no radical reaction appeared which would produce the cleavage of the vinyl-ether bond. So it seems that the plasmalogen alone was not able to generate radicals.

In order to evidence the antioxidant role of P_{PLM}OPE, UV-induced oxidation of P_{PLM}OPE/DLPC mixtures were realized in monolayer. For long-time irradiation, the $\Delta A_{30\ mN/m}$ of DLPC/P_{PLM}OPE mixtures were not quite different from those of DLPC/DMPC monolayers. But 30% mol P_{PLM}OPE delayed the beginning of the molecular area decrease for about 22 min, evidencing its antioxidant capacity (data not shown). Indeed, when a long-time irradiation was applied to the P_{PLM}OPE containing monolayer, too many radicals were generated and the P_{PLM}OPE molecules were not sufficient to impede the DLPC oxidation. For short UV-exposure time (15 min), inhibition of oxidation was observed in molecular area decrease rates as well as in lag times. $\Delta A_{30\ mN/m}$ of DLPC monolayers mixed with 30% mol DMPC was divided by 2, whereas with 30% mol P_{PLM}OPE the oxidation velocity was divided by 11 as compared to 10% mol DMPC and P_{PLM}OPE, respectively (Fig. 5A). The oxidation lag time of 30% mol P_{PLM}OPE monolayer was increased by about 470 min as compared to 30% mol DMPC (Fig. 5B). In monolayers, the threshold value determined for preventing oxidation under short UV-irradiation was about 25% mol P_{PLM}OPE.

Plasmalogens are known to be more vulnerable to oxidation than common diacyl phospholipids [15,16]. Moreover, they were consumed by the peroxyl radicals generated by the oxidation process of unsaturated phospholipids or DLPC that interact with the vinyl-ether function [16,22,43]. Murphy [13] suggested that a radical abstracts a hydrogen atom from the 1′-carbon atom position from the plasmalogen molecule and, further reaction with an oxygen molecule induces formation of a hydroperoxyl radical intermediate. In mixed DLPC/P_{PLM}OPE monolayers, the UV-irradiation induced the production of peroxyl radicals because plasmalogens impede the propagation rather than the initiation of phospholipids oxidation. So, in the first instants of the UV-irradiation in those monolayers, some peroxyl radicals generated by the DLPC UV-exposure react more rapidly with the plasmalogen vinyl-ether function than with other DLPC molecules. As described before, plasmalogens do not really inhibit polyunsaturated lipid oxidation but they act as a chain breaker by diverting the pathway to the vinyl-ether function [13]. Thus, when all the plasmalogen molecules are degraded, the peroxyl radicals generated are able to propagate to other DLPC acyl chains by a chain reaction. This is in accordance with the fact that the P_{PLM}OPE could not prevent the DLPC oxidation during long-time UV-irradiation, whereas for 15 min UV-irradiation, because it generated fewer radicals within the monolayer, P_{PLM}OPE molecules could trap these radicals. Thereby, the polyunsaturated phospholipids were degraded slowly and the UV-oxidation was delayed.

Plasmalogens could not have been recovered after oxidation because they are consumed during the antioxidative process. Plasmalogen degradation generated several molecules [13,44,45] and this complicated the composition of the mixture obtained after monolayer UV-irradiation.

The plasma membrane of eukaryote cells is organized in lipid rafts that resist cold detergent-extraction [46]. Pike et al. [11] described that lipid rafts are enriched in plasmenylethanolamine (26.9% of total phospholipids) and in arachidonic acid. The plasmenylethanolamine content described by Pike et al. [11] in rafts is in agreement with that found to have an antioxidant behavior in our work. In addition, it has been demonstrated that 35% cholesterol had an antioxidant effect, as evidenced by Girao et al. [9]. These peculiar membrane microdomains were found to be involved in membrane trafficking and signal transduction [47]. So, cholesterol and plasmalogens could have a protective role on microdomain lipids and proteins in order to preserve rafts functions. For example, arachidonic acid, a polyunsaturated fatty acid, is known to clearly participate in the free-radical propagation reactions [13].

Acknowledgements

We would like to thank Karim El Kirat for helpful discussions. This work was supported by the Centre National de la Recherche Scientifique and by a grant of the Région Rhone-Alpes.

References

[1] B.N. Pandey, K.P. Mishra, Radiation induced oxidative damage modification by cholesterol in liposomal membrane, Radiat. Phys. Chem. 54 (1999) 481–489.
[2] P.Y.Y. Wong, D.D. Kitts, Factors influencing ultraviolet and electron beam irradiation-induced free radical damage of ascorbic acid, Food Chem. 74 (2001) 75–84.
[3] T.B. Melo, G.S. Mahmoud, Radicals induced by illumination of a mixture of unsaturated fatty acids with ultraviolet light at 77 K, Magn. Reson. Chem. 26 (1988) 947–954.
[4] B. Bose, S. Agarwal, S.N. Chatterjee, Membrane lipid peroxidation by UV-A: mechanism and implications, Biotechnol. Appl. Biochem. 12 (1990) 557–561.
[5] M.-K. Shih, M.-L. Hu, Relative roles of metal ions and singlet oxygen in UVA-induced liposomal lipid peroxidation, J. Inorg. Biochem. 77 (1999) 225–230.
[6] G.F. Vile, R.M. Tyrrell, UVA radiation-induced oxidative damage to lipids and proteins in vitro and in human skin fibroblasts is dependent on iron and singlet oxygen, Free Radic. Biol. Med. 18 (1995) 721–730.
[7] P. Morliere, S. Salmon, M. Aubailly, A. Risler, R. Santus, Sensitization of skin fibroblasts to UVA by excess iron, Biochim. Biophys. Acta 1334 (1997) 283–290.
[8] X. Wang, P.J. Quinn, Vitamin E and its function in membranes, Prog. Lipid Res. 38 (1999) 309–336.
[9] H. Girao, C. Mota, P. Pereira, Cholesterol may act as an antioxidant in lens membranes, Curr. Eye Res. 18 (1999) 448–454.
[10] N. Nagan, R. Zoeller, Plasmalogens: biosynthesis and functions, Prog. Lipid Res. 40 (2001) 199–229.
[11] L.J. Pike, X. Han, K.N. Chung, R.W. Gross, Lipid rafts are enriched in arachidonic acid and plasmenylethanolamine and their composition is independent of caveolin-1 expression: a quantitative electrospray ionization/mass spectrometric analysis, Biochemistry 41 (2002) 2075–2088.

[12] R.W. Gross, High plasmalogen and arachidonic acid content of canine myocardial sarcolemma: a fast atom bombardment mass spectroscopic and gas chromatography-mass spectroscopic characterization, Biochemistry 23 (1984) 158–165.
[13] R.C. Murphy, Free-radical-induced oxidation of arachidonoyl plasmalogen phospholipids: antioxidant mechanism and precursor pathway for bioactive eicosanoids, Chem. Res. Toxicol. 14 (2001) 463–472.
[14] Y. Uemura, T.C. Lee, F. Snyder, A coenzyme A-independent transacylase is linked to the formation of platelet-activating factor (PAF) by generating the lyso-PAF intermediate in the remodeling pathway, J. Biol. Chem. 266 (1991) 8268–8272.
[15] O.H. Morand, R.A. Zoeller, C.R. Raetz, Disappearance of plasmalogens from membranes of animal cells subjected to photosensitized oxidation, J. Biol. Chem. 263 (1988) 11597–11606.
[16] D. Reiss, K. Beyer, B. Engelmann, Delayed oxidative degradation of polyunsaturated diacyl phospholipids in the presence of plasmalogen phospholipids in vitro, Biochem. J. 323 (1997) 807–814.
[17] M. Zommara, N. Tachibana, K. Mitsui, N. Nakatani, M. Sakono, I. Ikeda, K. Imaizumi, Inhibitory effect of ethanolamine plasmalogen on iron- and copper-dependent lipid peroxidation, Free Radic. Biol. Med. 18 (1995) 599–602.
[18] G. Jurgens, A. Fell, G. Ledinski, Q. Chen, F. Paltauf, Delay of copper-catalyzed oxidation of low density lipoprotein by in vitro enrichment with choline or ethanolamine plasmalogens, Chem. Phys. Lipids 77 (1995) 25–31.
[19] B. Engelmann, C. Brautigam, J. Thiery, Plasmalogen phospholipids as potential protectors against lipid peroxidation of low density lipoproteins, Biochem. Biophys. Res. Commun. 204 (1994) 1235–1242.
[20] K. El Kirat, F. Besson, A.F. Prigent, J.P. Chauvet, B. Roux, Role of calcium and membrane organization on phospholipase D localization and activity. Competition between a soluble and insoluble substrate, J. Biol. Chem. 277 (2002) 21231–21236.
[21] T. Viitala, J. Peltonen, UV-induced reaction kinetics of dilinoleoylphosphatidylethanolamine monolayers, Biophys. J. 76 (1999) 2803–2813.
[22] R.A. Zoeller, A.C. Lake, N. Nagan, D.P. Gaposchkin, M.A. Legner, W. Lieberthal, Plasmalogens as endogenous antioxidants: somatic cell mutants reveal the importance of the vinyl ether, Biochem. J. 338 (Pt 3) (1999) 769–776.
[23] Y. Rui, D.H. Thompson, Efficient stereoselective synthesis of plasmenylcholines, Chem. Eur. J. 2 (1996) 1505–1508.
[24] H.R. Pfaendler, V. Weimar, Synthesis of racemic ethanolamine plasmalogen, Synthesis, (1996) 1345–1349.
[25] M. Rejzek, M. Vacek, Z. Wimmer, A mild approach to the synthesis of *sn*-glycerol 1,2-di-γ-linolenate 3-palmitate, Helv. Chim. Acta 83 (2000) 2756–2760.
[26] G.L. Gaines, Insoluble Monolayers at Liquid–Gas Interfaces, Wiley Interscience, New York, 1966.
[27] X.M. Li, M. Ramakrishnan, H.L. Brockman, R.E. Brown, M.J. Swamy, *N*-myristoylated phosphatidylethanolamine: interfacial behavior and interaction with cholesterol, Langmuir 18 (2002) 231–238.
[28] J.T. Davies, E.K. Rideal, Interfacial phenomena, Academic Press, New York, 1963.
[29] J.M. Smaby, M.M. Momsen, H.L. Brockman, R.E. Brown, Phosphatidylcholine acyl unsaturation modulates the decrease in interfacial elasticity induced by cholesterol, Biophys. J. 73 (1997) 1492–1505.
[30] D. Marsh, Lateral pressure in membranes, Biochim. Biophys. Acta 1286 (1996) 183–223.
[31] J.C. Maziere, J.D. Routier, C. Maziere, R. Santus, L.K. Patterson, Diphenylhexatriene (DPH)-labeled lipids as a potential tool for studies on lipid peroxidation in monolayer films, Free Radic. Biol. Med. 22 (1997) 795–802.
[32] J. Smaby, A. Hermetter, C. Schmid, F. Paltauf, H. Brockman, Packing of ether and ester phospholipids in monolayers. Evidence for hydrogen-bonded water at *sn*-1 acyl group of phosphatidylcholines, Biochemistry 22 (1983) 5808–5813.
[33] J.H. Pak, V.P. Bork, R.E. Norberg, M.H. Creer, R.A. Wolf, R.W. Gross, Disparate molecular dynamics of plasmenylcholine and phosphatidylcholine bilayers, Biochemistry 26 (1987) 4824–4830.
[34] X.L. Han, R.W. Gross, Plasmenylcholine and phosphatidylcholine membrane bilayers possess distinct conformational motifs, Biochemistry 29 (1990) 4992–4996.
[35] P. Demediuk, D.L. Cowan, E.A. Moscatelli, Effects of plasmenylethanolamine on the dynamic properties of the hydrocarbon region of mixed phosphatidylcholine-phosphatidylethanolamine aqueous dispersions. A spin label study, Biochim. Biophys. Acta 730 (1983) 263–270.
[36] G. Subbanagounder, A.D. Watson, J.A. Berliner, Bioactive products of phospholipid oxidation: isolation, identification, measurement and activities, Free Radic. Biol. Med. 28 (2000) 1751–1761.
[37] G.K. Marathe, S.M. Prescott, G.A. Zimmerman, T.M. McIntyre, Oxidized LDL contains inflammatory PAF-like phospholipids, Trends Cardiovasc. Med. 11 (2001) 139–142.
[38] S.P. Gabbita, D.A. Butterfield, K. Hensley, W. Shaw, J.M. Carney, Aging and caloric restriction affect mitochondrial respiration and lipid membrane status: an electron paramagnetic resonance investigation, Free Radic. Biol. Med. 23 (1997) 191–201.
[39] B. Bose, S.N. Chatterjee, Correlation between UVA-induced changes in microviscosity, permeability and malondialdehyde formation in liposomal membrane, J. Photochem. Photobiol., B 28 (1995) 149–153.
[40] M. Choe, C. Jackson, B.P. Yu, Lipid peroxidation contributes to age-related membrane rigidity, Free Radic. Biol. Med. 18 (1995) 977–984.
[41] D.M. Hawcroft, P.A. Martin, Studies on age related changes in the lipids of mouse liver microsomes, Mech. Ageing Dev. 3 (1974) 121–130.
[42] J.W. Borst, N.V. Visser, O. Kouptsova, A.J. Visser, Oxidation of unsaturated phospholipids in membrane bilayer mixtures is accompanied by membrane fluidity changes, Biochim. Biophys. Acta 1487 (2000) 61–73.
[43] P.J. Sindelar, Z. Guan, G. Dallner, L. Ernster, The protective role of plasmalogens in iron-induced lipid peroxidation, Free Radic. Biol. Med. 26 (1999) 318–324.
[44] N. Khaselev, R.C. Murphy, Structural characterization of oxidized phospholipid products derived from arachidonate-containing plasmenyl glycerophosphocholine, J. Lipid Res. 41 (2000) 564–572.
[45] S. Stadelmann-Ingrand, S. Favreliere, B. Fauconneau, G. Mauco, C. Tallineau, Plasmalogen degradation by oxidative stress: production and disappearance of specific fatty aldehydes and fatty alpha-hydroxyaldehydes, Free Radic. Biol. Med. 31 (2001) 1263–1271.
[46] D.A. Brown, J.K. Rose, Sorting of GPI-anchored proteins to glycolipid-enriched membrane subdomains during transport to the apical cell surface, Cell 68 (1992) 533–544.
[47] A. Rietveld, K. Simons, The differential miscibility of lipids as the basis for the formation of functional membrane rafts, Biochim. Biophys. Acta 1376 (1998) 467–479.